SUPPORTING INFORMATION

Ant assemblages have darker and larger members in cold environments

Tom R. Bishop, Mark P. Robertson, Heloise Gibb, Berndt J. van Rensburg, Brigitte Braschler, Steven L. Chown, Stefan H. Foord, Caswell T. Munyai, Iona Okey, Pfarelo G. Tshivhandekano, Victoria Werenkraut and Catherine L. Parr

Appendix S1 Colour assignment.

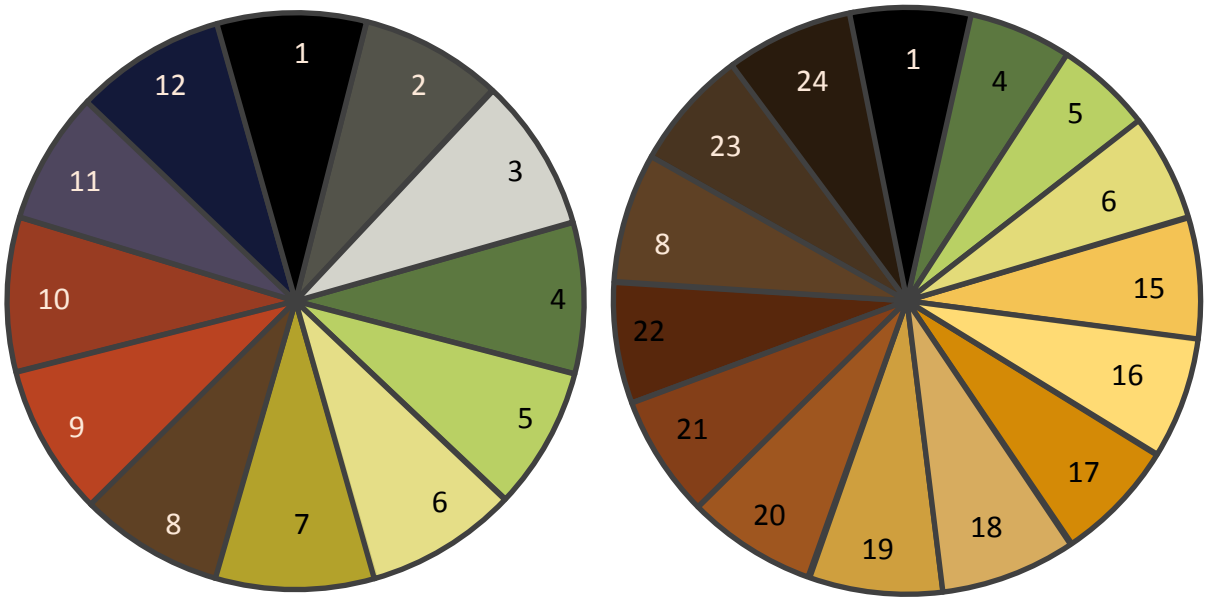

Fig S1.1. Colour wheels used to categorise the colour of ant species across the three continents.

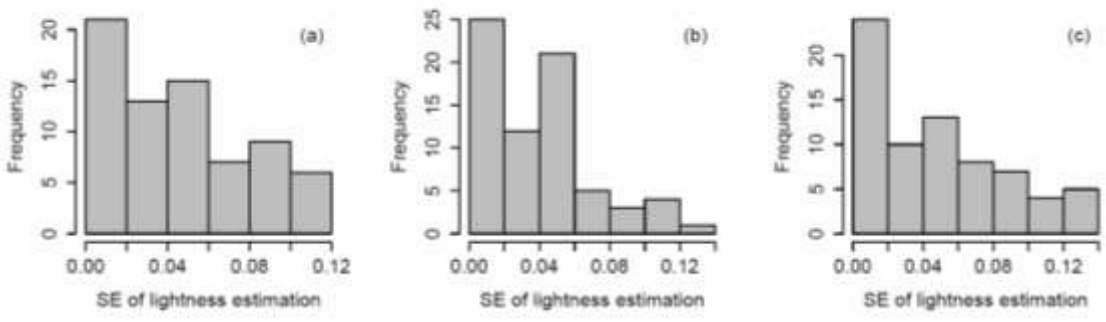

Fig S1.2. Histograms showing the standard errors of lightness values estimated for the (a) head, (b) mesosoma and (c) gaster by the five observers used in this study on a set of 71 photographs of ants from antweb.org. Mean standard error for the head is 0.04, mesosoma is 0.036, and gaster is 0.045.

Appendix S2 Multivariate imputation using chained equations (MICE) of MacDonnell Ranges body size.

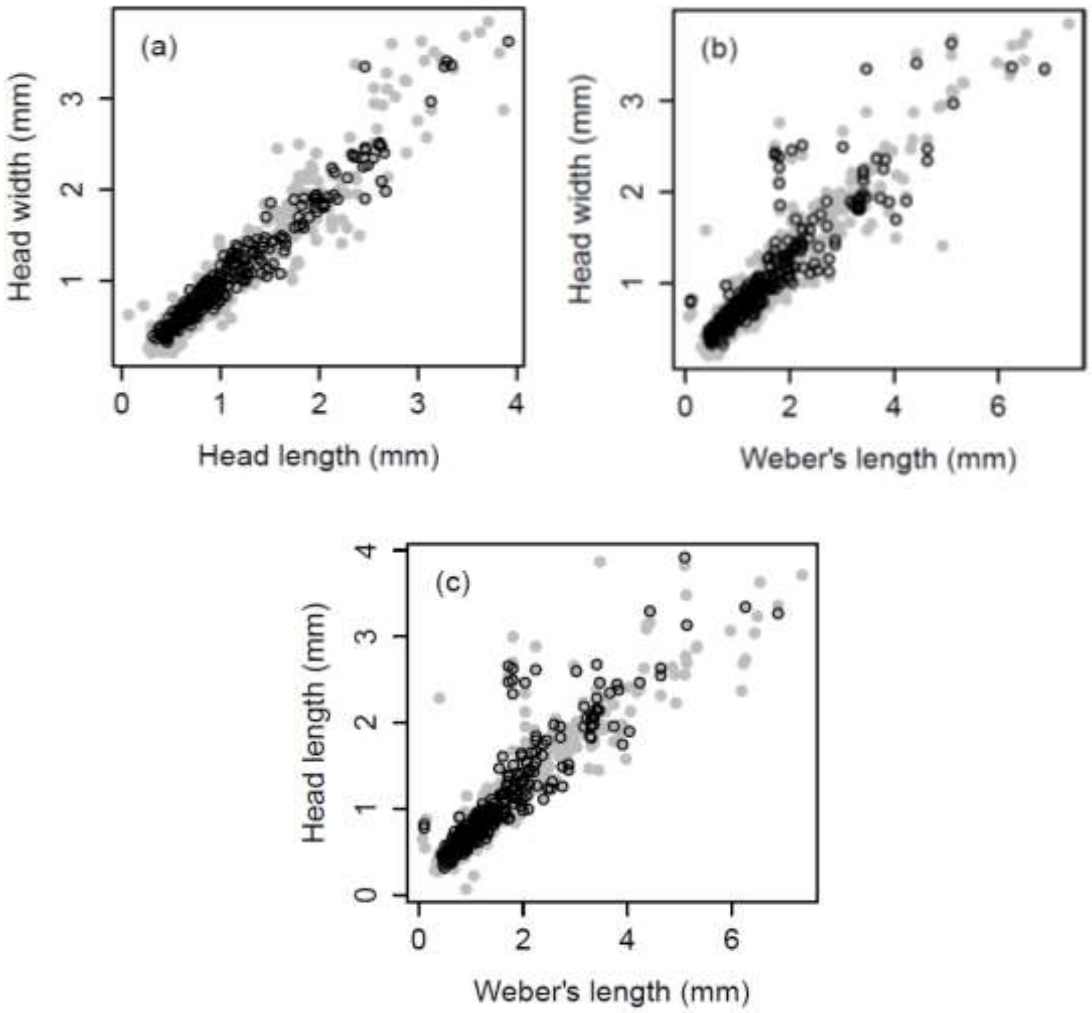

Fig S2.1 Plots showing relationship between morphological traits for Australian ants from the Snowy Mountains, MacDonnell Ranges and Ben Lomond Plateau, Tasmania. Values for the MacDonnell Ranges ants are circled in black. For plots (b) and (c) the Weber's length values (x-axis) for the MacDonnell species (black circles) were estimated using MICE.

Appendix S3 Phylogenetic signal.

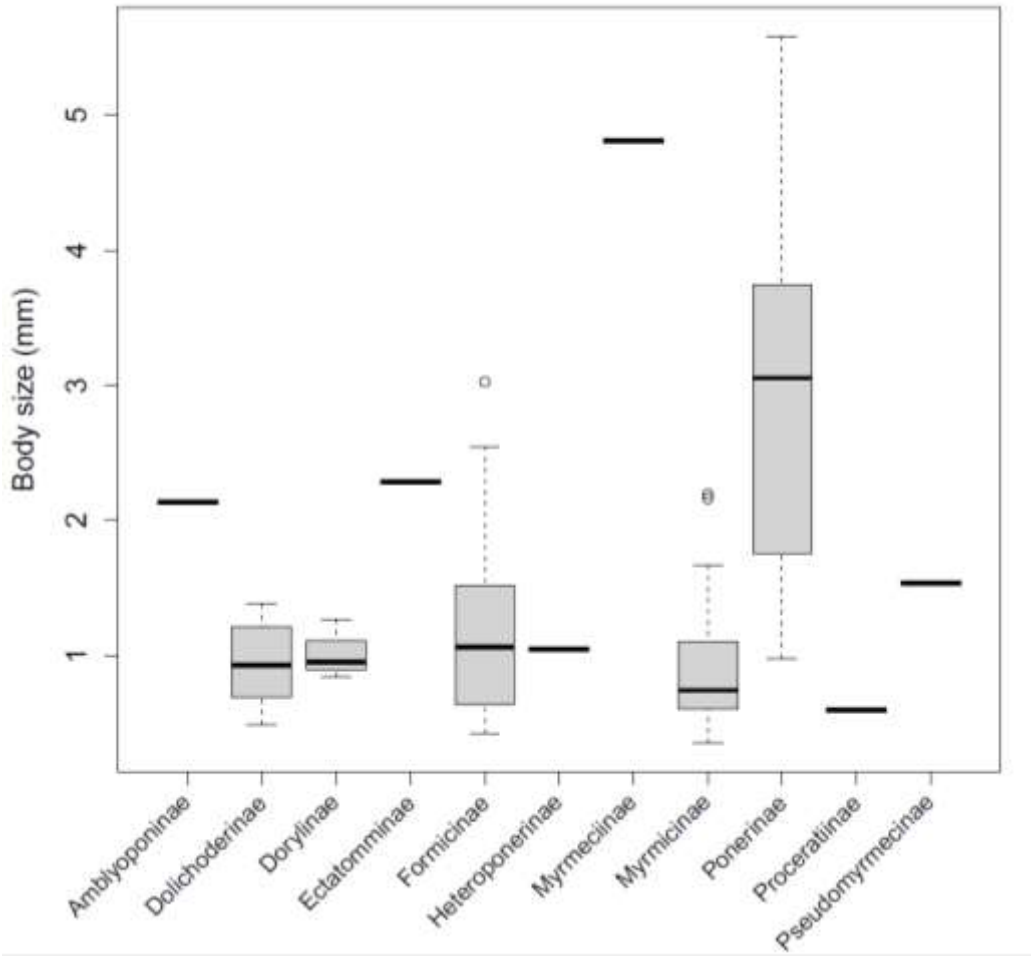

Fig S3.1. Plot showing the distribution of average genus body sizes across the ant subfamilies present in this study.

Appendix S4 Relationship between temperature values obtained from data loggers in the Maloti-Drakensberg, Soutpansberg and Patagonian Andes and those extracted from *WorldClim*.

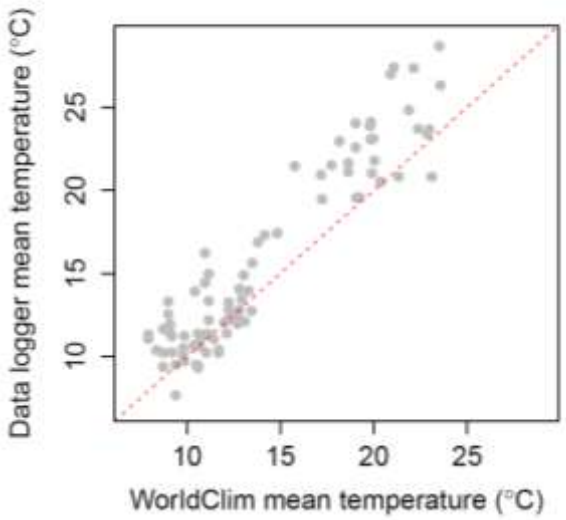

Fig S4.1. Relationship between temperature values obtained from data loggers and those extracted from *WorldClim*, (r = 0.94, p < 0.001). Red line indicates a 1:1 relationship.

Appendix S5 Species richness effects.

The distribution of lightness is not evenly spread across the species in the dataset (Fig. S5.1). This may produce biased results if sampling effects occur and influence the lightness value of assemblages. For example, an assemblage may be dark in colour simply because a large proportion of the species able to colonise it are themselves dark.

A linear mixed model (LMM) of assemblage lightness as a function of assemblage species richness was run. The random effects structure was the same as that for the spatial model in the main text: transect was nested within mountain range within continent. The effect of species richness was significant according to a type III Wald χ^2 test ($\chi^2 = 5.62$, $p = 0.02$) and had a positive influence (Fig. S5.2) on assemblage lightness but actually explained very little variation in assemblage lightness ($R^2_m = 0.02$, $R^2_c = 0.38$). This small R^2_m suggests that richness does not have a large influence on assemblage lightness patterns.

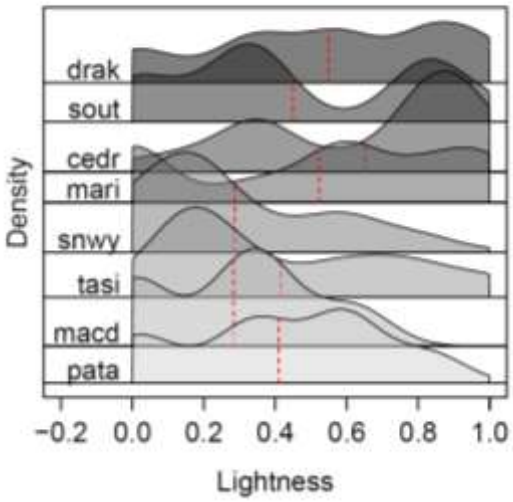

Fig S5.1 Stacked density plot showing the distribution of lightness values for each mountain range. Underlying data is at the morphospecies level. Bandwidth used was 0.1. Codes and number of species as follows: drak = Maloti-Drakensberg (n = 92); sout = Soutpansberg (n = 129); cedr = Cederberg (n = 94); mari = Mariepskop (n = 92), snwy = Snowy Mountains (n = 109); tasi = Ben Lomond plateau, Tasmania (n = 12); macd = MacDonnell Ranges (n = 49); pata = Andes, North West Patagonia (n = 15).

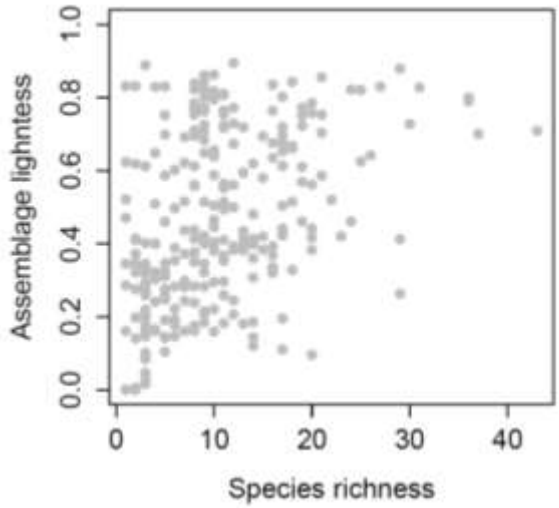

Fig S5.2 Plot showing the relationship between assemblage lightness and species richness.

Appendix S6 Modelling of lightness across space using *microclim* temperature data.

Data

Soil temperatures at 1 cm above the soil under 0% shade were extracted from the *microclim* dataset (Kearney *et al.*, 2014). A single average was calculated per sampling grid using data from January to March.

Data loggers vs microclim

There was a strong and significant positive correlation between data logger temperature values and *microclim* estimates ($r = 0.92$, $p < 0.001$, Fig. S6.1). Major axis regression showed that the intercept was greater than zero (95% CIs intercept = 1.12, 3.62) and the slope was slightly less than one (95% CIs slope = 0.76, 0.91).

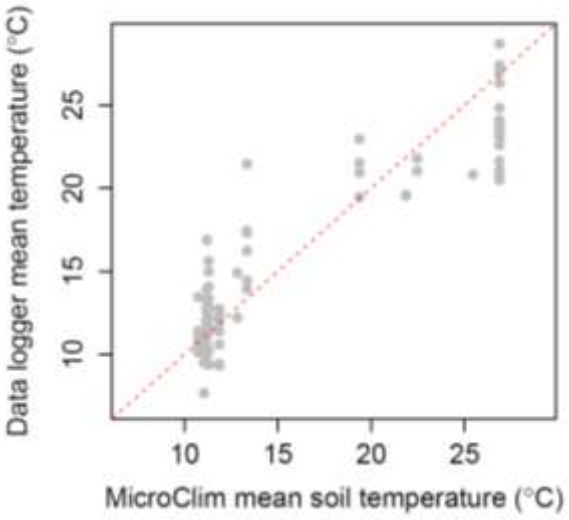

Fig S6.1. Relationship between temperature values obtained from data loggers and those extracted from micro*clim*, ($r = 0.92$, $p < 0.001$). Red line indicates a 1:1 relationship.

Modelling

Spatial modelling took place as described in the main text. Linear mixed models (LMMs) were used to assess how much variation in assemblage weighted lightness could be explained by *microclim* estimates of temperature, amount of UV-B radiation and assemblage weighted body size. This was done using the lme4 package in R (Bates *et al.*, 2014). An interaction term between temperature and UV-B was also fitted. All explanatory variables were scaled and standardised in order to allow greater interpretability of the regression coefficients (Schielzeth, 2010). Explanatory variables were coded as second order orthogonal polynomials in order to detect curvature in the relationships between them and assemblage weighted lightness. A nested random effects structure of transect within mountain range within continent was used to account for geographic configuration of the study sites. The response variable of assemblage weighted lightness was logit transformed to meet Gaussian assumptions. An information theoretic approach was used to assess models with different

combinations of the explanatory variables. Bias corrected Akaike's information criterion (AICc) values were used to compare models. Marginal (due to fixed effects only) and conditional (due to fixed effects and random effects) R^2 values were calculated for each model (Bartoń, 2013; Nakagawa & Schielzeth, 2013). Type III tests using Wald χ^2 statistics were used to assess the significance of the predictors in the "best" model. Each of the 274 observations in this analysis was an independent assemblage of ants.

The best model was the same as when using *WorldClim* data. It contained the main effects of temperature, UV-B, body size and also included an interaction between temperature and UV (Table S6.1). All variables were significant according to type III Wald X2 tests (Table S6.2). Assemblage weighted lightness declined with increasing assemblage weighted body size (Fig. S6.2a). At low levels of UV-B, assemblage weighted lightness increased with increasing temperature. At high levels of UV-B there was a hump-shaped relationship between lightness and temperature - at higher temperatures lightness declined (Fig. S6.2b).

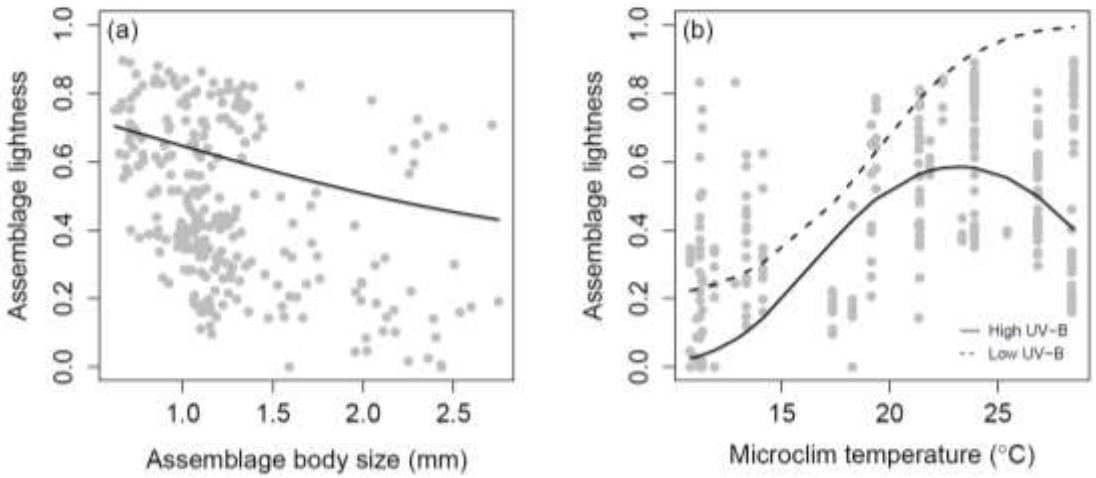

Fig S6.2. Plots showing the relationship between assemblage lightness and body size (a) and average microclim derived summer temperature (b). Lines display model predictions. In (b), solid line represents predictions for low levels of UV-B, dashed line represents predictions for high UV-B (n = 274).

Table S6.1. Comparative and summary statistics for linear mixed models explaining variation in ant assemblage colour across space. Predictors were all second order orthogonal polynomials and included average body size (BS + BS^2), average summer temperature (T + T^2) and average UV-B radiation (UV + UV^2). The temperature variables were derived from *microclim*. Listed are the degrees of freedom (d.f.), maximum log-likelihood (LL), Akaike's bias corrected information criterion (AICc) and it's change relative to the top ranked model (ΔAICc), the model probabilities (wAICc) and the marginal and conditional R^2s. Marginal R^2 (R^2m) is the amount of variation explained by the fixed effects, conditional R^2 (R^2_c) is that explained by the fixed and random effects.

Model	d.f.	LL	AICc	ΔAICc	wAICc	R^2_m	R^2_c
Spatial							
~ (BS + BS^2) + (T + T^2) X (UV + UV^2)	15	-321.19	674.25	0.00	0.90	0.50	0.53
~ (BS + BS^2) + (T + T^2) + (UV + UV^2)	11	-328.40	679.80	5.55	0.06	0.46	0.62
~ (BS + BS^2) + (T + T^2)	9	-330.82	680.32	6.08	0.04	0.48	0.70
~ (T + T^2) X (UV + UV^2)	13	-330.46	688.32	14.07	0.00	0.38	0.51
~ (T + T^2) + (UV + UV^2)	9	-336.42	691.52	17.27	0.00	0.33	0.58
~ (T + T^2)	7	-338.83	692.07	17.82	0.00	0.42	0.68
~ (BS + BS^2)	7	-347.08	708.58	34.33	0.00	0.07	0.41
~ (BS + BS^2) + (UV + UV^2)	9	-346.38	711.44	37.19	0.00	0.21	0.42
~ 1	5	-356.71	723.64	49.39	0.00	0.00	0.44
~ (UV + UV^2)	7	-356.50	727.41	53.17	0.00	0.01	0.41

Table S6.2. Test statistics (χ^2), degrees of freedom (d.f.) and p values from type III Wald tests on the best spatial model (top ranked from Table S6.1). Explanatory variables were second order orthogonal polynomials and included average body size (BS + BS^2), average summer temperature (T + T^2) and average UV-B radiation (UV + UV^2). The temperature variables were derived from microclim.

Spatial	χ^2	d.f.	p
T + T^2	16.04	2	<0.001
UV + UV^2	15.80	2	<0.001
BS + BS^2	20.17	2	<0.001
(T + T^2) X (UV + UV^2)	35.86	4	<0.001

Appendix S7 Modelling of lightness across space for common and rare species.

Table S7.1. Comparative and summary statistics for linear mixed models explaining variation in ant assemblage colour across space for either common or rare species. Predictors were all second order orthogonal polynomials and included average body size (BS + BS^2), average summer temperature (T + T^2) and average residual UV-B radiation (UV + UV^2). Assemblage lightness and body size were recalculated for common and rare models separately. Common species in assemblages were those that made up to 90% of the individuals. Rare species were the remainder. Listed are the degrees of freedom (d.f.), maximum log-likelihood (LL), Akaike's bias corrected information criterion (AICc) and it's change relative to the top ranked model (ΔAICc), the model probabilities (wAICc) and the marginal and conditional R^2s. Marginal R^2 (R^2_m) is the amount of variation explained by the fixed effects, conditional R^2 (R^2_c) is that explained by the fixed and random effects.

Common species	d.f.	LL	AICc	ΔAICc	wAICc	R^2_m	R^2_c
~ (BS + BS^2) + (T + T^2) X (UV + UV^2)	15	-326.12	684.27	0.00	0.98	0.47	0.69
~ (BS + BS^2) + (UV + UV^2)	9	-337.26	693.27	8.99	0.01	0.22	0.70
~ (BS + BS^2) + (T + T^2) + (UV + UV^2)	11	-335.82	694.74	10.46	0.01	0.29	0.65
~ (T + T^2) X (UV + UV^2)	13	-342.03	711.60	27.33	0.00	0.13	0.71
~ (BS + BS^2) + (T + T^2)	9	-346.45	711.64	27.37	0.00	0.35	0.69
~ (UV + UV^2)	7	-350.73	715.93	31.66	0.00	0.10	0.72
~ (T + T^2) + (UV + UV^2)	9	-350.31	719.37	35.10	0.00	0.09	0.68
~ (T + T^2)	7	-355.53	725.52	41.25	0.00	0.20	0.68
~ (BS + BS^2)	7	-364.22	742.90	58.63	0.00	0.05	0.60
~ 1	5	-370.62	751.49	67.22	0.00	0.00	0.66
Rare species							
~ (BS + BS^2) + (UV + UV^2)	9	-322.72	664.16	0.00	0.47	0.15	0.47
~ (BS + BS^2) + (T + T^2) X (UV + UV^2)	15	-316.59	665.12	0.96	0.29	0.17	0.54
~ (BS + BS^2) + (T + T^2) + (UV + UV^2)	11	-322.09	667.24	3.08	0.10	0.16	0.46
~ (BS + BS^2)	7	-326.56	667.56	3.40	0.09	0.13	0.45
~ (BS + BS^2) + (T + T^2)	9	-325.09	668.89	4.73	0.04	0.14	0.45
~ (UV + UV^2)	7	-342.69	699.82	35.66	0.00	0.04	0.42
~ (T + T^2) + (UV + UV^2)	9	-342.18	703.06	38.91	0.00	0.06	0.41
~ 1	5	-348.90	708.04	43.88	0.00	0.00	0.40
~ (T + T^2)	7	-346.83	708.11	43.95	0.00	0.03	0.41
~ (T + T^2) X (UV + UV^2)	13	-340.79	709.03	44.88	0.00	0.06	0.46

Table S7.2. Test statistics (χ^2), degrees of freedom (d.f.) and p values from type III Wald tests on the best spatial models for common and rare species subsets (top ranked from Table S7.1). Explanatory variables were second order orthogonal polynomials and included average body size (BS + BS^2), average summer temperature (T + T^2) and average residual UV-B radiation (UV + UV^2).

Common	χ^2	d.f.	p
T + T^2	18.49	2	<0.001
UV + UV^2	1.19	2	0.55
BS + BS^2	39.81	2	<0.001
(T + T^2) X (UV + UV^2)	21.67	4	<0.001
Rare			
BS + BS^2	74.44	2	<0.001
UV + UV^2	7.86	2	0.02

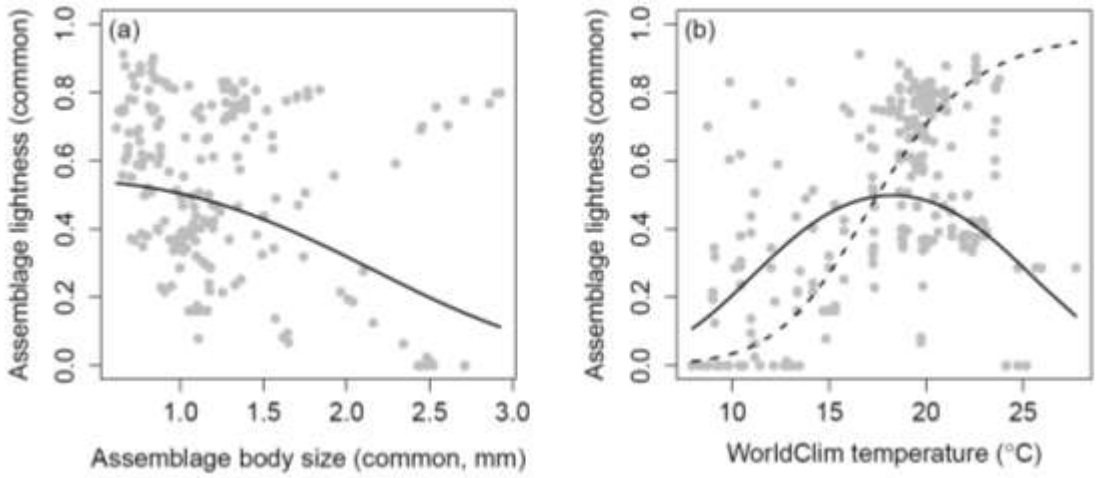

Fig S7.1 . Plots showing the relationship between assemblage lightness and body size (a) and average *WorldClim* derived summer temperature (b). Only common species were used in the calculation of lightness and body size in plots (a) and (b). Lines display model predictions. In (b), solid line represents predictions for low levels of UV-B, dashed line represents predictions for high UV-B.

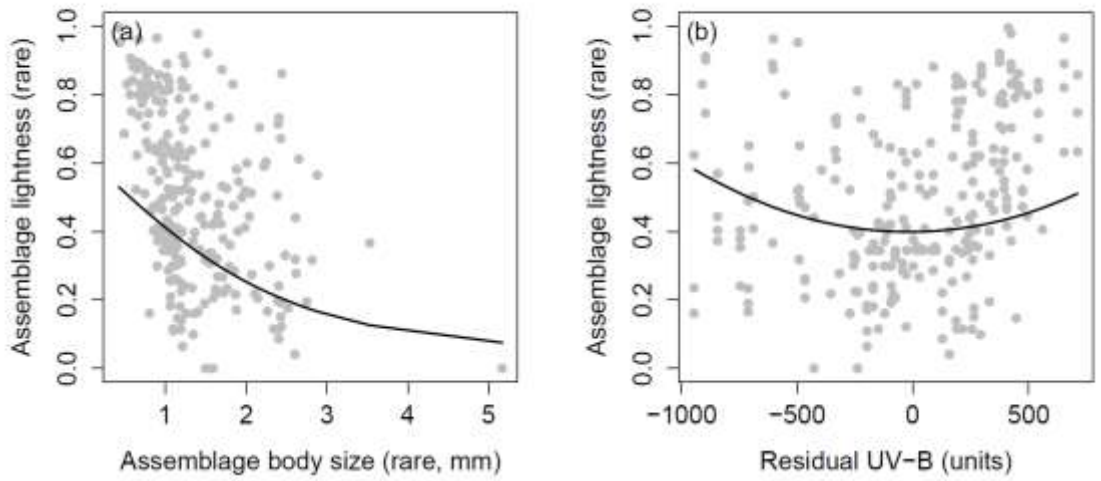

Fig S7.2 . Plots showing the relationship between assemblage lightness and body size (a) and residual summer UV-B (b). Only rare species were used in the calculation of lightness and body size in plots (a) and (b). Lines display model predictions.

References

Bartoń, K. (2013) *MuMIn: Multi-model inference*.

Bates, D., Maechler, M., Bolker, B., Walker, S., Christensen, R.H.B., Singmann, H. & Dai, B. (2014) *lme4: Linear mixed-effects models using Eigen and S4*.

Kearney, M.R., Isaac, A.P. & Porter, W.P. (2014) microclim: Global estimates of hourly microclimate based on long-term monthly climate averages. *Scientific data*, **1**

Nakagawa, S. & Schielzeth, H. (2013) A general and simple method for obtaining R^2 from generalized linear mixed-effects models. *Methods in Ecology and Evolution*, **4**, 133-142.

Schielzeth, H. (2010) Simple means to improve the interpretability of regression coefficients. *Methods in Ecology and Evolution*, **1**, 103-113.